A Technoeconomic Assessment of Solar Energy to Supplement Urban Heat Networks

Mark Reynolds
Graduate Engineer, FairHeat
mark.reynolds@fairheat.com

Abstract

Heat pump led heat networks will be a key feature of the UK's future energy strategy, with c.20% of heat forecast to be delivered via heat networks and with many likely to utilise heat pump technologies.

This electrification of heat will place a significant additional burden on grid infrastructure.

Utilising rooftop photovoltaic (PV) or solar thermal technologies could help to reduce the grid electricity load on these heat pump led systems. Since roof-space in urban environments is often small compared to the network demand size, it is unclear which technology would provide the best outputs, carbon reductions and lifetime cost benefit, especially in relation to changing demand profiles resulting from the UK's response to COVID-19.

A technoeconomic feasibility assessment has been carried out on the usage of PV and solar thermal as supplementary technologies on different sized heat networks in the London area.

The model found that increasing PV capacity had a larger effect on reducing both carbon emissions and total system cost over 30-years than solar thermal.

Despite this, the model also found that increasing air source heat pump (ASHP) capacity gives the largest carbon emissions reduction whilst simultaneously reducing upfront capital expenditure (CapEx) due to the reduction of the carbon offsetting costs between 80% and 95% heat fractions.

Consequently, maximising the performance of the heat pump before considering PV capacity is advised. Achieving a >95% ASHP heat fraction with rooftop PV was found to provide the most optimal carbon and cost reductions on any scheme.

Keywords

Solar Thermal, Photovoltaics (PV), Air Source Heat Pump (ASHP), Boiler, Heat Network

1.0 Introduction

The UK Climate Change Committee (CCC) released the 6th carbon budget in December 2020 which outlines a roadmap to net zero by 2050 in accordance with the Paris Agreement of 2016. As part of the strategy for decarbonising heat in buildings, the report predicts that the use of low carbon heat via communal and district heating networks is likely to provide at least 20% of all UK heat by 2050, a significant increase from the 2% currently provided [1].

It also states that the use of low carbon heat from sources such as air source and ground source heat pumps (ASHP and GSHP respectively) are likely to provide the central generation technology to reduce and eventually remove the dependency on natural gas in favour of electrification. This paper considers only the use of ASHPs.

An important factor in the design of heat pump-led heat networks is ensuring operation at lower temperatures to maximise the annual or seasonal coefficient of performance (COP or SCOP) and consequently reduce electricity demand, and therefore the costs passed through to connected residents.

Fourth generation heat networks minimise the losses from low temperature hot water (LTHW) systems and enable centralised heat pumps to operate at 55-60 °C [2], without boosting required within premises for domestic hot water (DHW). There are a number of these schemes already operating within the London area. For the purposes of this paper, a 60/30 heat network is assumed.

Using a heat pump to supply the system peak loads and 100% of the heat fraction can result in high upfront CapEx. Instead, a hybrid solution using gas boilers as peak plant and thermal storage to maximise the heat pump run hours can be utilised to maintain a high heat pump heat fraction and optimise between CapEx and operating expenditure (OpEx).

It is currently estimated that an 80% heat pump heat fraction is the minimum required heat fraction to comply with carbon reduction requirements in the London Plan [3] and Part L of building regulations [4] [5], assuming gas peaking boilers for the remaining 20% heat fraction.

As heat networks are technology agnostic, different supplemental technologies can be considered to determine the most feasible operational strategy to move towards net-zero.

The usage of both solar thermal and photovoltaics have emerged as low-cost renewable technologies to decarbonise heat and power. PV has played a significant role in decarbonising both domestic and grid electricity with the UK installed capacity reaching over 13.5 GW in February 2021 [6]. Similarly, solar thermal powered heat networks can be used in conjunction with interseasonal storage to provide low cost and low carbon heat, this has been clearly demonstrated by several schemes in Denmark, most notably the 110 MWth array in Silkeborg supplying 20% of annual heat demand to 21,000 connected users [7].

Nevertheless, it is unclear whether the reduced available roof space on urban heat networks will be sufficient for either PV to supplement heat pump electricity consumption, or solar thermal to supplement the network heat load.

As it is likely that either technology will reduce the carbon emissions of the scheme and affect the amount of boiler top-up required, the effects of carbon offset payments required by the Greater London Authority (GLA) and the preference of top up boilers between gas and electric boilers should be considered.

Furthermore, in response to the COVID-19 pandemic, greater time spent at home and increased flexibility in our daily heat demand routine may have caused demand profiles to change. This may result in higher demand during the day and therefore matching the times when solar resource is available.

Consequently, there is a clear need to investigate the performance, economic viability, and carbon emissions of different supplemental solar technologies in both our pre- and mid- pandemic demand patterns.

This paper calculates the technoeconomic feasibility of building and operating 4th generation heat networks with different supplemental generation strategies by creating an hourly load model based on averaged weather data and existing schemes in London.

An ASHP and gas boiler strategy sized to provide 80% and 20% of the heat demand, respectively is used as the counterfactual base case from which to compare the following alternatives:

- The effect of adding rooftop PV
- The effect of adding rooftop solar thermal
- The effect of increasing ASHP size instead of using either PV or solar thermal
- The effect of using electric boilers rather than gas on the above outputs
- The effect of pre- and mid-pandemic demand profiles on the above outputs
- The effect of scheme size on the above outputs.

2.0 Methodology

2.1. Basic heat network detail assumptions

All scenarios modelled in this paper are assumed to be in line with a 4th generation, 2-pipe heat network serving Heat Interface Units (HIUs) which provide space heating via underfloor heating (UFH) and domestic hot water within dwellings. No commercial connections have been allowed for in any case. The following assumptions have also been made for all modelled scenarios.

- Boilers, thermal stores, and ancillaries will be sited in the energy centre at basement level, the ASHP and solar arrays (either PV or solar thermal) will be sited at roof level.
- All schemes are fed from one central energy centre. As such, solar thermal and the ASHP will be limited to installation on the energy centre rooftop (which is assumed to be the largest) to minimise additional piping and controls complexity issues associated with multiple rooftop arrays. This is believed to be a realistic assumption from a developer's perspective, however, the additional costs and complexities have not been modelled in this paper.
- All solar arrays have been modelled as fixed-tilt; PV systems are grid-connected with no allowance for battery storage.
- All roof space is available for heating plant. No allowance has been made for lift overruns, chilled plant, or Air Handling Units (AHU's) which are sometimes located at roof level.
- All calculations are based on the CIBSE Test Reference Year (TRY) weather data for London [8].

The system temperatures have been kept the same in all scenarios and are given in Table 1 below.

Location	Value (°C)
Network flow temperature	60
Avg network return temperature	30
ASHP flow temperature	55
Boiler flow temperature	60
Solar thermal flow temperature	70
Space heating 'on' temperature	12

Table 1 – Temperature inputs for each scenario.

2.2. Building types

Analysis was carried out on both existing and 'in-design' heat networks in purpose-built blocks of flats in London. Five were selected that are believed to be representative of the existing variation in scheme architectures and rooftop availabilities, these are given in Table 2 below.

Location	Dwellings	Blocks/Roof tops	Total available roof space (m^2)	Available roof space for PV (m^2)	Available roof space for ST/ ASHP (m^2)
Tower Hamlets	100	1	625	625	625
Southwark	200	1	600	600	600
Newham	350	2	1,360	1,360	1,020
Newham	500	8	2,800	2,800	450
Kingston upon Thames	1,000	>10	c.6,550	6,550	940

Table 2 – Building details and rooftop availabilities

These schemes will be used as reference scheme to determine the impact of load size and rooftop availability on technology option feasibility.

2.3. Annual demands, heat losses, and plant sizing

The total annual demands for space heating and DHW have been averaged from design calculations according to SAP 10.1 methodology on heat networks in London across typical 1-bed, 2-bed, and 3-bed flats [9]. An average ratio of 5:4:1 respectively of each dwelling type was calculated and applied to the total annual demands to determine average loads per flat.

These were calculated to be 2,317 and 2,201 kWh/dwelling/year for DHW and space heating, respectively.

A constant value of 0.06 kW/dwelling was used for network losses based on a multi-riser system in compliance with CP1 2020 [2], and a constant 0.03 kW/dwelling losses were used for HIU standby losses as per BESA HIU test results [10] [2].

An ASHP was selected from a well-known global manufacturer, who provided COP data based on target outlet temperature and ambient temperature. Using this and the demand profiles explained below, the ASHP was sized to provide an 80% heat fraction. Thermal storage was sized based on observed available energy centre space in each scheme and was maximised where possible.

The combined annual loads and sizing details are given in Table 3 below.

Location	Dwellings	Annual dwelling demand (kWh)	Annual network losses (kWh)	Annual HIU losses (kWh)	HP size (kW)	TS size (m^3)	HP Heat fraction (%)
Tower Hamlets	100	451,660	43,800	26,280	65	20	81%
Southwark	200	1,043,480	87,600	52,560	130	20	80%
Newham	350	1,580,820	153,300	91,980	230	30	81%

Newham	500	2,258,310	219,000	131,400	320	40	80%
Kingston upon Thames	1000	4,516,620	262,800	438,000	650	50	80%

Table 3 – Annual demands, losses, and plant sizing details

2.4. Demand profiles

2.4.1. Domestic hot water diversity

To distribute the demands in Table 3 throughout the year, hourly diversity profiles have been calculated from operational heat network data of 337 dwellings in one of the above schemes which is known to have a high occupancy percentage. To ensure reliability, the profiles were calculated and compared between 2020 and 2019.

The data was taken from June 1st to July 31st in both years to ensure only DHW demand was being observed. The heat losses of the system were assumed to be the minimum average load between the hours of 03:00 -05:00 AM when the system is at minimum load. This was then negated from the overall hourly averages to analyse the true DHW hourly demand. The resulting profiles are given in Figure 1 (a-d).

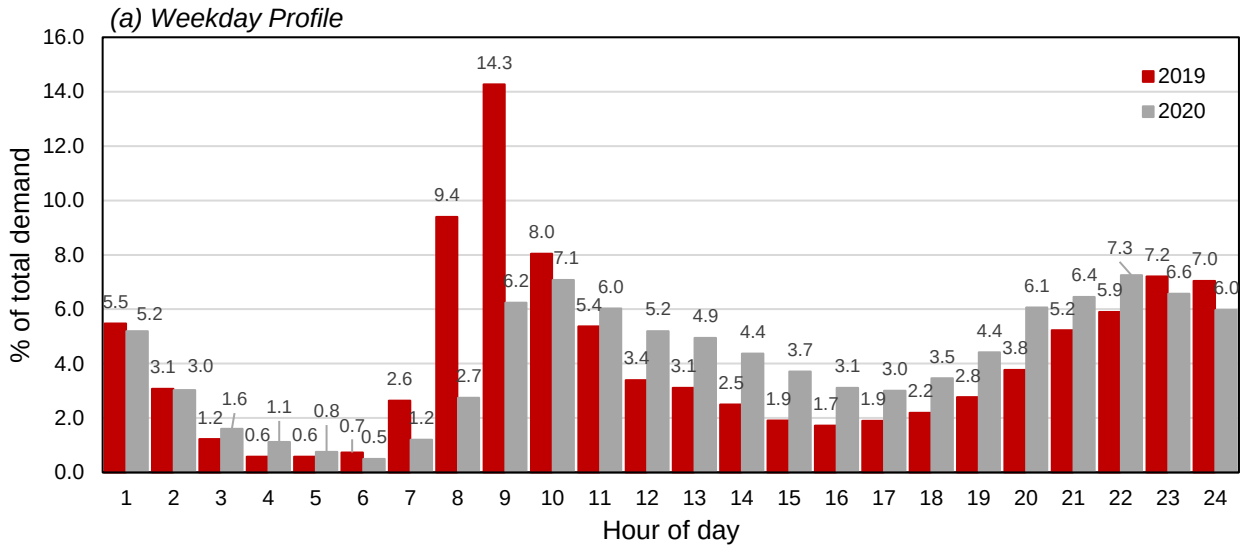

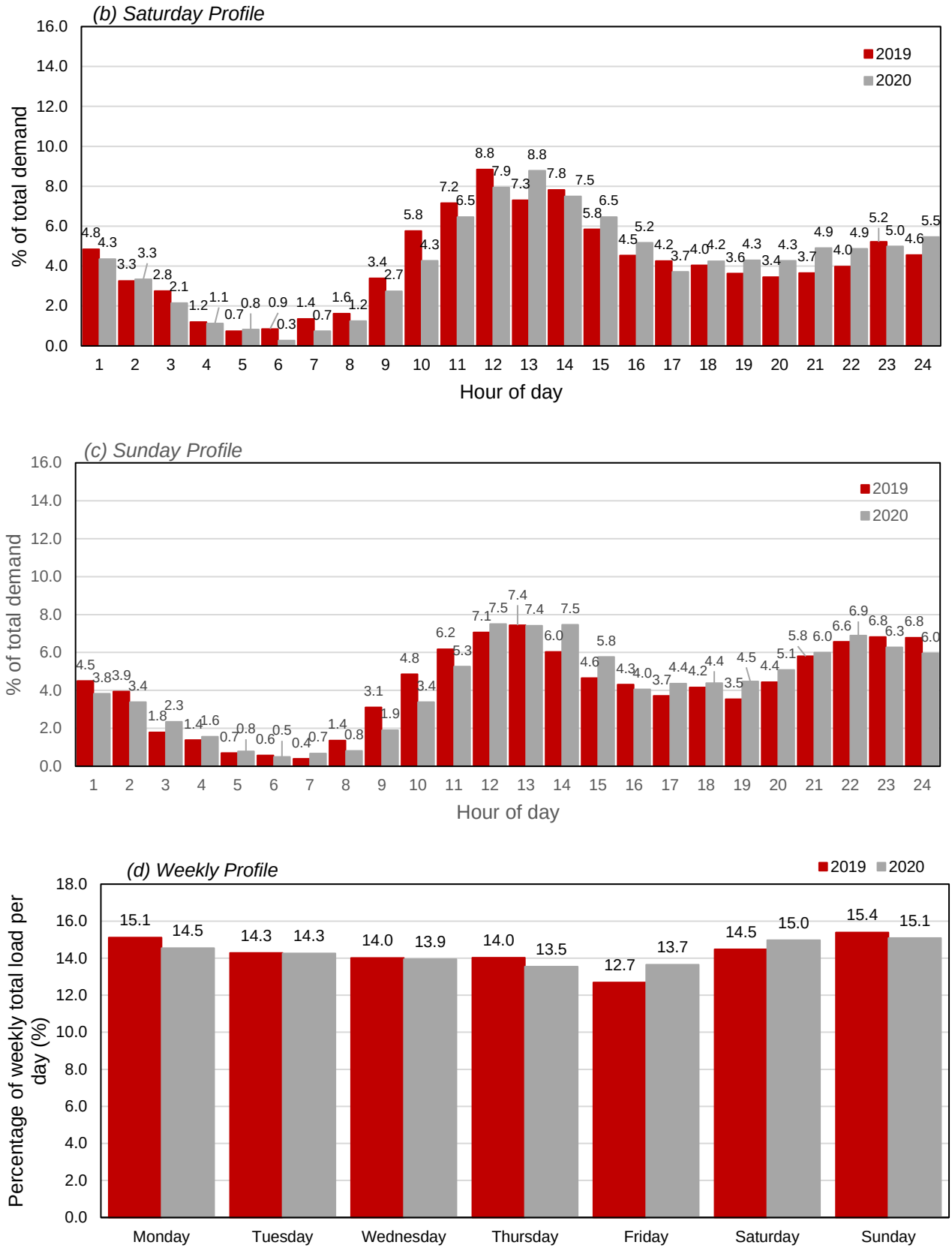

Figure 1 – (a-d) calculated DHW profiles using heat meter data for 337 dwellings.

There is a clear difference in the weekday profiles for each year. 2020 shows a much smaller morning peak and increased demand throughout the day. This behaviour could

be attributed to the effect of the COVID-19 pandemic resulting in more home working and greater flexibility in demand times. The Saturday and Sunday profiles are largely similar in magnitude but with slightly time-shifted peaks to an hour later in the day.

The percentage of demand throughout the week is similar on each day for each year, however there is a 1% increase in demand on Fridays in 2020, which could also be a result of COVID-19 and the restricted availability to leave home on Fridays.

The overall weekly consumption increased by 11.6% in 2020 which is a marked rise and could be attributed to residents taking all their showers at home and working from home during the day; this demand might previously have been used in gyms or offices. This change in demand would need further analysis and consequently, the annual consumption is assumed to be the same for all models in this paper.

Both profiles are used in the modelling to determine the effect on heat fractions and total system cost.

The hourly demand is calculated using the above profiles and is adjusted using the monthly DHW factors in Table 1c in SAP 10.1 [9].

2.4.2. Space heating diversity

The hourly profile assumes a portion of the dwellings use heating when the ambient temperature is less than 12 °C which is the space heating ‘on’ temperature, as described in Table 1.

A factor has been included within the model to account for this portion of dwellings which have their space heating on for each hour and month of the year. For example it has been assumed only 10 % of people will require heat when the ambient temperature falls below 12 °C at midnight in July, whereas it is assumed that all residents will have their heating on under the same circumstances in winter.

This factor is multiplied by the degree difference between 12 °C and the ambient temperature during that hour (degree hours). The magnitude of heat use per dwelling for that hour is then calculated by multiplying the degree hours in that hour by the annual space heating demand per dwelling and dividing by the total number of degree hours in the year.

These assumptions have had to be made due to the lack of referenceable space heating diversity data published and the uncertainty from deriving it from the data sets used above. However, comparisons of the outputs from this hourly load model to actual consumption data from operational heat network schemes have shown the combined hourly load profiles to closely match each other, providing confidence that the diversity values accurately reflect reality.

2.5. Generation profiles

2.5.1. Technology hierarchy

The model meets the hourly demand by prioritising low carbon technologies and maximising the usage of thermal storage. Solar thermal is always prioritised for each hour as outlined in decision tree 1. Any demand that cannot be met by solar thermal will pass through to the ASHP and boilers outlined in decision tree 2. Boilers (gas or electric) are used as a last resort technology when peak demands cannot be met by combinations of either solar thermal, ASHP or thermal stores.

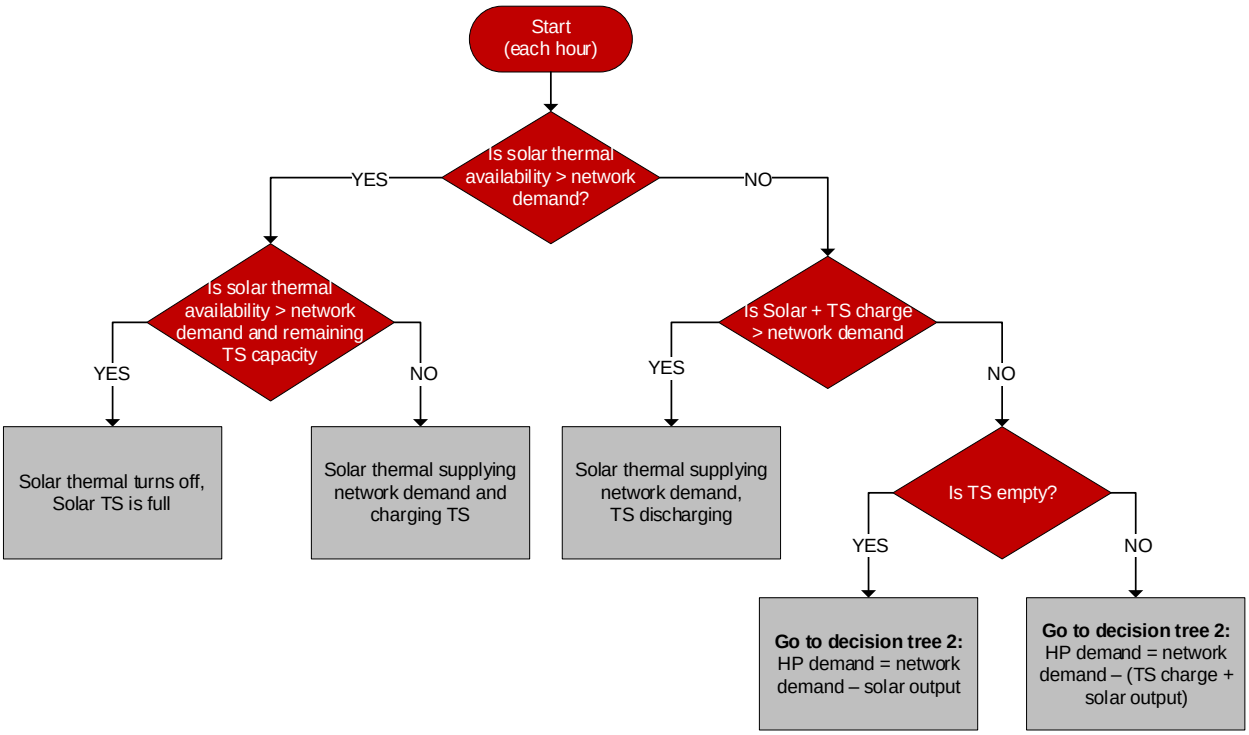

Figure 2 – Decision tree 1, outlining solar thermal operating modes.

Since the solar thermal evacuated tubes chosen in this study have the ability to be left stagnant and not reach dangerously high temperatures, the solar thermal array is disabled in circumstances where the thermal store is full and the output is greater than the demand. Once turned off in that day, the solar thermal array cannot be enabled until the first hour of the next day to enable cooling.

Decision tree 2, given in Figure 3, determines how excess demand can be met by HP's and boilers.

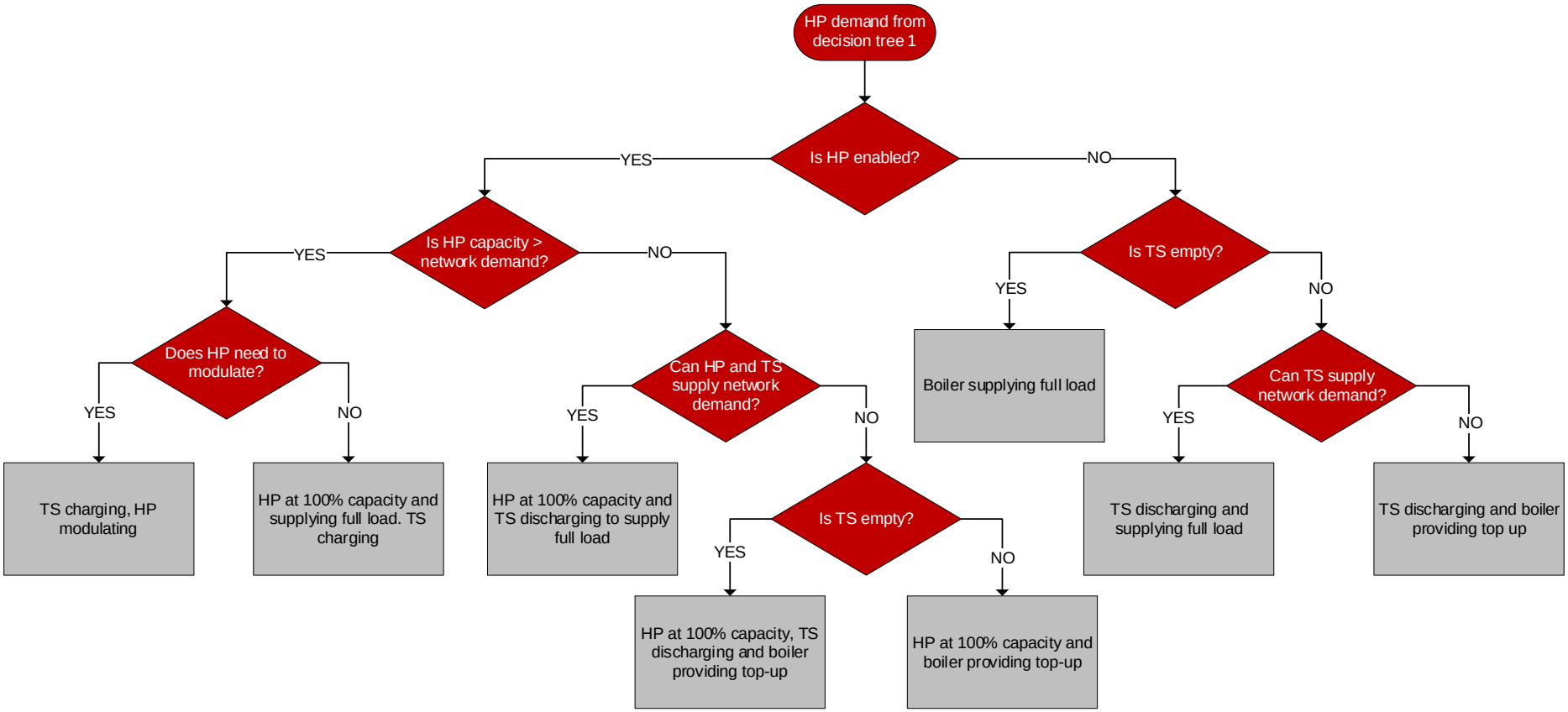

Figure 3 – Decision tree 2, outlining HP and boiler operating modes.

2.5.2. Solar Availability

2.5.2.1. Transposition model

The isotropic sky model using the view factors proposed by Liu & Jordan (1963) [11] has been chosen due to its simplicity and accuracy, this is given in equation 1 below.

$$I_{GTI} = I_B(R_B) + I_D(R_D) + I_{GHI}\left[\rho_g(R_R)\right] \quad (1)$$

Where, I_{GTI} is global tilted irradiation (W/m^2), I_B is beam horizontal irradiation (W/m^2), I_D is diffuse horizontal irradiation (W/m^2) I_{GHI} is global horizontal irradiation (W/m^2) and ρ_g is the albedo coefficient. The albedo has been assumed to be 0.2 for all cases as a rough approximation [12] [13].

R_B, R_D and R_R are the geometric view factors for beam, diffuse and reflected irradiance, respectively. These are given by equations 1.1 – 1.3.

$$R_B = \frac{Cos(\theta)}{Cos(\theta_z)} \quad (1.1)$$

$$R_D = \frac{1 + Cos(\beta)}{2} \quad (1.2)$$

$$R_R = \frac{1 - Cos(\beta)}{2} \quad (1.3)$$

Where β is the tilt angle (°), θ_Z is the solar zenith angle (°) and θ is the angle of incidence (AOI) of the sun's irradiance on the tilted plane (°). The cosine of the AOI is given by equation 1.4 below.

$$Cos(\theta) = Cos(\theta_z)\, Cos(\beta) + Sin(\theta_z)\, Sin(\beta)\, Cos(\gamma_s - \gamma) \quad (1.4)$$

Where γ_s is the solar azimuthal angle (°) and γ is the panel azimuthal angle (°). By substituting equations 1.1-1.4 into equation 1, the irradiation reaching the tilted plane can be calculated for each hour of the irradiance data.

2.5.2.2. Array Orientation

The tilt angle β and panel azimuthal angle γ were varied from 0° to 65° and -45° (SE) to 45° (SW) respectively to find the panel orientation which maximized the incoming irradiance. The optimum angles were found to be 30° tilt and 0° azimuth (due South) for the CIBSE TRY weather data set for London. This resulted in an annual tilted incident irradiation of 1027 kWh/m^2/yr. These angles were retained in each modelled scenario for both PV and solar thermal.

2.5.2.3. Shading and panel spacing

The row spacing was calculated to ensure that no panel shading would occur during the hours of 10AM to 2PM (4-hour winter solar window) on the winter solstice. Using the optimum tilt angle of 30° and a minimum solar altitude angle of 10°, the row spacing was calculated to be 2.83 m. Panel shading was therefore assumed negligible during peak sun hours and no additional shading from adjacent buildings was considered.

2.5.2.4. Solar thermal profile

An industry standard evacuated tube solar collector panel with a similar size to the PV panel was chosen from a well-known global manufacturer. The performance details are given in Table 4.

Parameter	**Value**
Gross area (m^2)	2.36
Absorber area (m^2)	1.51
Aperture area (m^2)	1.6
Optical efficiency (η_0 - %)	75.2
Heat loss factor (a_1 – W/m^2.K)	1.906
Heat loss factor (a_2 – W/m^2.K)	0.006
Maximum stagnation temperature (°C)	150
Thermal Capacity (C_{eff} – kJ/m^2.K)	5.97
Incidence Angle Modifier (K_θ – dimensionless)	0.98

Table 4 – Evacuated tube solar collector manufacturer data

The collector has been modelled using the steady state model as detailed in the test standards EN 12975 [14], ASHRAE 93-77 [15] and now more recently in EN ISO 9806 [16]. Used both widely in testing and simulation, the energy balance, if expressed as an output power can be given as in equation 2.

$$Q_{ST} = A\,[I_{GTI}\,(K_\theta)\eta_0 - [a_1(T_m - T_a)] - [a_2(T_m - T_a)^2] - C_{eff}] \quad (2)$$

Where, Q_{ST} is the solar collector heat output (W), A is the collector aperture area (m^2), K_θ is the incidence angle modifier, η_0 is the optical efficiency (%), $a_1$is the first order heat loss factor (W/m^2.K), a_2 is the second order heat loss factor (W/m^2.K), T_m is the mean collector temperature (°C) and C_{eff} is the thermal capacity (J/m^2.K).

The solar collector set point was set to target an output temperature of 70°C to allow for a 10°C approach temperature on a plate heat exchanger (PHE) when charging the thermal store.

This methodology produced a total annual output availability of 493 kWh/ m^2 of aperture area.

2.5.2.5. Photovoltaic profile

An industry standard 72-cell monocrystalline-Si PV panel was chosen from a well-known global manufacturer which had the following performance details.

Parameter	**Value**

Aperture area (m^2)	2.08
Gross area (m^2)	2.21
Nominal maximum power (P_{nom} – W)	400
Module efficiency at STC ($\eta_{mp,STC}$ - %)	20.1
Power temperature coefficient at P_{nom} (α_P - %/°C)	-0.35
Nominal operating cell temperature ($T_{C,NOCT}$ - °C)	42 ± 3

Table 5 – Monocrystalline PV module manufacturer data.

The power output of the PV array was calculated using the relationship defined in equation 3 as outlined in Duffie & Beckman (2013) [17].

$$P_{PV} = P_{nom} f_{PV} \left(\frac{I_{GTI}}{I_{STC}}\right)\left[1 + \alpha_P\left(T_c - T_{c,STC}\right)\right] \quad (3)$$

Where P_{PV} is power output (W), P_{nom} is the rated capacity of the array (W), I_{STC} is the incident irradiation under standard test conditions (STC) (1000 W/m^2), α_P is the power temperature coefficient at P_{nom} (%/°C), $T_{C,STC}$ is the PV cell temperature under STC (25°C) and T_c is the PV cell temperature calculated at each time step (°C).

f_{PV} in the above equation is the derating factor or performance ratio (%). This accounts for both balance of system (BOS) losses including DC/AC cable losses and inverter losses, and 'other' losses including soiling/dust and panel mismatch. A combined derating factor of 88% is used to account for this as recommended in the PVOUT calculations for medium-size commercial installations on SOLARGIS maps available on Global Solar Atlas [18]. This factor is assumed constant for all scenarios.

The cell temperature T_c for each hour can be calculated using equation 3.1 [17] [19] which makes the assumption that the PV array is operating at its maximum power point (MPP), and the efficiency can be taken as such.

$$T_C = \frac{T_a + \frac{\left(T_{C,NOCT} - T_{a,NOCT}\right)I_{GTI}}{I_{T,NOCT}}\left(1 - \frac{\eta_{mp,STC}\left(1 - \alpha_p T_{C,STC}\right)}{\tau\alpha}\right)}{1 + \frac{\left(T_{C,NOCT} - T_{a,NOCT}\right)I_{GTI}}{I_{T,NOCT}}\left(\frac{\alpha_P \eta_{mp,STC}}{\tau\alpha}\right)} \quad (3.1)$$

Where T_a is the ambient temperature (°C), $T_{C,NOCT}$ is the nominal operating cell temperature (NOCT) (°C), $T_{a,NOCT}$ is the ambient temperature at which NOCT is calculated (20°C), $I_{T,NOCT}$ is the irradiation at which NOCT is calculated (800 W/m^2), $\eta_{mp,STC}$ is the efficiency at MPP under STC. $\tau\alpha$ is the transmittance and absorptance respectively of the cover over the PV modules (%). This factor is assumed to be 0.9 In all cases as outlined in Duffie & Beckman [17] which does not introduce significant error.

The methodology above produced an annual PV output of 907 kWh/ kW_p which is used in all models.

2.6. Carbon emissions

The carbon emission calculations use the emissions factors for mains gas and grid electricity defined in Table 12 and 12d respectively in SAP 10.1 (2019) [9]. These are believed to be an accurate representation of a decarbonising grid over the modelled period.

Gas emissions are calculated for each hour of the model using equation 4 below

$$Gas\ Emissions\ (kgCO_2) = GCF_{SAP} \times \frac{Q_{GB}}{\eta_{GB}} \quad (4)$$

Where GCF_{SAP} is the gas carbon factor (kg CO_2/ kWh), Q_{GB} is the hourly heat output of the gas boiler (kWh) and η_{GB} is the gas boiler efficiency assumed to be 85% for all scenarios.

Electricity emissions are also calculated hourly using a similar methodology in equation 5.

$$Electricity\ Emissions\ (kgCO_2) = ECF_{SAP} \times [(P_{HP} + P_{EB} + P_{ANC}) - P_{PV}] \quad (5)$$

Where ECF_{SAP} is the electricity carbon factor (kg CO_2/ kWh) P_{HP} is heat pump electricity consumption (kWh) P_{EB} is electric boiler electricity consumption (kWh) and P_{ANC} is energy centre ancillary electricity consumption which is assumed to be a constant 5kW each hour to allow for energy centre control systems and pumps.

P_{HP} and P_{EB} are calculated using equations 5.1 – 5.2.

$$P_{HP} = \frac{Q_{HP}}{COP_{HP}} \quad (5.1)$$

$$P_{EB} = \frac{Q_{EB}}{\eta_{EB}} \quad (5.2)$$

Where Q_{HP} is the heat pump heat output (kWh), COP_{HP} is the heat pump coefficient of performance (COP), Q_{EB} is the electric boiler heat output (kWh) and η_{EB} is the electric boiler efficiency, assumed to be 99% in all scenarios.

The heat pump COP is selected from the ASHP manufacturer data based on ambient temperature and target outlet temperature for each hour.

Since the electricity carbon emissions are considered net, PV electricity supplying the heat pump has no carbon emission associated and exported PV electricity has a negative carbon emission.

2.7. Area requirements

The area requirements are calculated as the sum of the total solar array size including panel spacing, and the total ASHP size with manufacturers clearance requirements. A 5% uplift has been added for access and egress.

2.8. Financial conditions

2.8.1. Capital Costs

Linear cost factors have been used to determine the installed cost for the selected energy strategy in each scenario. These are detailed in Table 6.

Installed capital cost	**Rounded Cost**	**Reference**
ASHP (£/kW)	700	Manufacturer guideline
Monocrystalline-Si PV (£/kW)	1,070	BEIS, Solar PV cost data, 2020 [20]
Evacuated tube (£/m^2 gross)	33**0**	Manufacturer guideline
Gas Boiler (£/kW)	80	Manufacturer guideline
Electric Boiler (£/kW)	65	Manufacturer guideline
Carbon offset payment (£/tonne CO_2)	95	GLA, The London Plan, 2021 [3]

Table 6 – Capital cost factors

As the schemes investigated are relatively small scale, the economies of scale are assumed not to be significant.

The carbon offset payment for schemes in London payable to the Greater London Authority (GLA) is also included in the capital cost of each scheme.

2.8.2. Operating Costs

Linear operating costs have also been used to determine the utility consumption and maintenance costs of each technology, these are given below in Table 7.

Operating cost	**Rounded Cost**	**Reference**
Electricity import tariff (£/kWh)	0.12	UK quarterly energy prices [21]
Electricity export tariff (£/kWh)	0.05	Tariff disclosed from private developer
Gas tariff (£/kWh)	0.03	UK quarterly energy prices [21]
ASHP maintenance (£/kW/year)	11.00	Manufacturer guideline
Monocrystalline-Si PV maintenance (£/kW/year)	10.00	NREL/IRENA models [22], [23]
Evacuated tube maintenance (£/m^2 gross/year)	10.00	Assumed same as PV, validated with maintenance contractor charge out of £80/hr.
Gas Boiler maintenance (£/kW/year)	3.50	Manufacturer guideline

Electric Boiler maintenance (£/kW/year)	3.00	Manufacturer guideline

Table 7 – Operating cost factors

Electricity and gas prices are inflated annually based on BEIS energy price projections [24]; maintenance costs are inflated annually using an average 2% inflation rate.

2.8.3. NPV

The net present value (NPV) of the generation CapEx and OpEx costs have been calculated over a period of 30 years assuming a discount rate of 3.5%. NPV is calculated using equation X.

$$NPV = \sum_{t=0}^{n} \frac{CF_n}{(1+i)^n} \quad (6)$$

Where CF_t is the annual cash flow (£), i is the discount rate (%) and n is the number of years.

For each year, the outputs and loads are assumed to be the same, in reality a small reduction in output would occur with the PV due to light and elevated temperature induced degradation (LeTID), however, this has not been accounted for year-on-year and no replacements have been considered.

3.0 Results and discussion

For sections 3.1 to 3.4, the results provided have been calculated using the 350-dwelling scheme as an example and the DHW demand profiles have been assumed to be in line with data gathered from 2019 to show pre-pandemic behaviour. The effect of changing these profiles and size of scheme has been analysed in sections 3.5 and 3.6.

3.1. Effect of increasing PV capacity

Based on the roof space availability given in Table 2, and the plant sizing details given in Table 3, the results for increasing the PV capacity on the base case scheme with heat pump and gas boilers sized for 80% and 20% respective heat fractions are given below.

	Base case	**Scenario 1 (Half roof)**	**Scenario 2 (Full roof)**
Array sizing results			
Number of PV Panels	0	105	210
PV Capacity (kW_p)	0	42	84
PV Utilization (%)	0	100	91
Total roof area requirement (m^2)	26	683	1,340
Financial/ performance results			
Total installed CapEx (£)	£ 708,577	£ 739,616	£ 770,656
Net annual OpEx (£)	£ 83,818	£ 79,674	£ 75,958
Electricity import (kWh)	567,665	529,673	497,792
Gas import (kWh)	432,253	432,253	432,253
Total carbon emissions (kg CO_2)	173,192	168,212	163,231
Total System Cost (£ NPV)	£ 2,383,437	£ 2,337,038	£ 2,299,058
Delivered Cost of Heat (£/kWh)	£ 0.043	£ 0.040	£ 0.038

Table 8 – Modelling results of increased PV provision on 350-unit scheme.

The model suggests that the addition of PV to the rooftop decreases the total system cost. After investigation of the sensitivity of array size, it was found that this trend continues until the PV array is large enough to be achieving less than a c. 40% utilization factor, at which point increasing array size begins to increase total system cost again. It is important to note that the 40% utilization factor could not be achieved on any scheme due to roof space availability. Consequently, a ‘full roof’ array offered the lowest cost and lowest carbon on every scheme size.

The key driver this finding is the reduction in electricity consumption which results in significantly reduced operational costs over 30 years and a small reduction in carbon emissions.

The revenue created from exporting PV to the grid had very little effect on NPV, for the 350-dwelling scheme, scenario 2 generated only £340 per annum due to the high utilization resulting from the heat pump consumption, even without the use of a battery which was not considered in any scenario.

As the PV array does not affect the boiler top-up required, the heat fractions remain constant, as does the gas consumption.

3.2. Effect of increasing solar thermal capacity

The results of increasing the solar thermal capacity on the base case scheme with heat pump and gas boilers sized for 80% and 20% respective heat fractions are given below.

	Base case	**Scenario 1 (Half roof)**	**Scenario 2 (Full roof)**
Array sizing results			
Number of solar thermal panels	0	98	200
Gross panel area (m^2)	0	231	472
Total roof area requirement (m^2)	26	677	1356
Financial/ performance results			
Total installed CapEx (£)	£ 708,577	£ 771,399	£ 836,401
Net annual OpEx (£)	£ 83,818	£ 83,067	£ 82,308
Electricity import (kWh)	567,665	548,703	528,693
Gas import (kWh)	432,253	420,937	409,618
Total carbon emissions (kg CO_2)	173,192	168,453	163,581
Total System Cost (£ NPV)	£ 2,383,437	£ 2,438,760	£ 2,496,638
Delivered Cost of Heat (£/kWh)	£0.043	£0.041	£0.040

Table 9 – Modelling results of increased solar thermal provision on 350-unit scheme.

Unlike PV, increasing solar thermal increases total system costs. This is largely because the solar thermal array cannot generate enough heat to have a meaningful impact on heat fraction due to the small space allocation as can be seen from Figure 4 below.

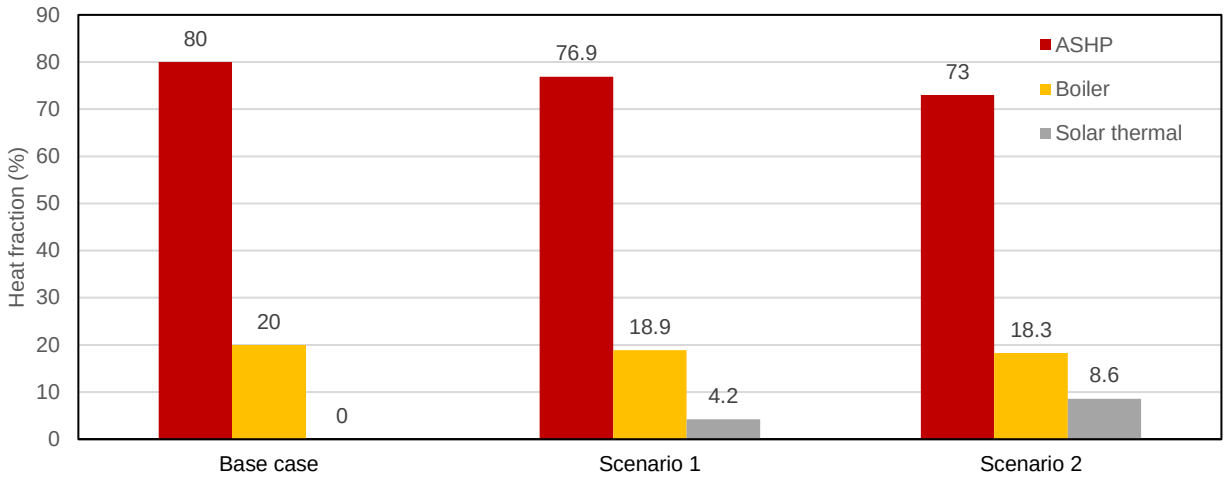

Figure 4 – Impact of increasing solar thermal size on heat fraction for a 350-unit scheme.

A maximum 8.6% heat fraction is achieved using the maximum available space in scenario 2. Furthermore, solar thermal has a much bigger effect on reducing the heat pump heat fraction (7% reduction against the base case) than it does on reducing the boiler heat fraction (1.7% reduction against the base case). This is because the peak demands still need to be supplied by boilers as they are happening at times where there is little solar availability, and the heat pump is only providing the low-grade heat at 55 °C.

Solar thermal is ultimately less favourable than PV because PV had a greater impact on reducing the cost of electricity import which in turn has a greater effect on operational costs. In the case of solar thermal, the simultaneous reduction in gas and electricity is not significant enough to recoup its additional upfront CapEx. The lower reduction in gas and electricity also results in marginally higher carbon emissions with solar thermal.

3.3. Effect of increasing ASHP capacity

An alternative strategy for reducing carbon emissions would be to simply increase heat pump capacity as compared to the addition of PV or solar thermal.

The results of increasing the heat pump capacity on the base case scheme with heat pump and gas boilers sized for 80% and 20% respective heat fractions are given below. None of the following scenarios include either PV or solar thermal.

	Base case	**90% heat fraction**	**95% heat fraction**	**97.5% heat fraction**	**100% heat fraction**
Heat pump sizing results					
Heat pump size (kW)	230	300	360	400	580
Heat pump heat fraction (%)	80.4	89.8	95.2	97.6	100

Total roof area requirement (m^2)	26	33	40	44	64
Financial/ performance results					
Total installed CapEx (£)[1]	£ 708,577	£ 661,636	£ 646,294	£ 649,007	£ 712,416
Net annual OpEx (£)	£ 83,818	£ 87,829	£ 90,487	£ 91,792	£ 93,447
Electricity import (kWh)	567,665	639,421	682,983	702,073	725,559
Gas import (kWh)	432,253	227,292	106,501	55,070	-
Total carbon emissions (kg CO_2)	173,192	141,494	123,058	115,308	107,514
Total System Cost (£ NPV)	£ 2,383,437	£ 2,392,858	£ 2,416,982	£ 2,440,307	£ 2,530,234
Delivered Cost of Heat (£/kWh)	£ 0.043	£ 0.044	£ 0.046	£ 0.046	£ 0.047

1 - Note capital costs do not consider grid infrastructure upgrade costs for gas or electricity.

Table 10 – Modelling results of increased heat pump provision on 350-unit scheme.

The model shows there is a reduction in CapEx from 80% to 95% ASHP heat fraction, which is due to the reduced GLA carbon offsetting costs from the effect of the lower emissions. Although this does not reduce total system cost, it does reduce the rate of increase until upwards of 95% where the carbon emissions reductions diminish and the CapEx costs rise sharply. This is mainly due to increased electrical consumption of the heat pump at high heat fractions.

Additionally, the total system cost only increases by 2.5% between 80% and 95% heat fractions whilst simultaneously reducing carbon emissions by 29%. Therefore there is a significant incentive to settle for a slightly higher system cost and higher resident tariff in favour of significantly lower carbon emissions without having to supply the full peak load from the heat pump.

3.4. Effect of using an electric boiler

In the interest of examining schemes which are fully electric, the effect of using electric boilers in comparison to gas boilers has also been modelled.

The results of changing between gas boilers and electric boilers have been shown by modelling NPV and carbon emissions with different plant sizes for the same scheme. This is given in Figure 5(a) and (b). None of the following scenarios include either PV or solar thermal.

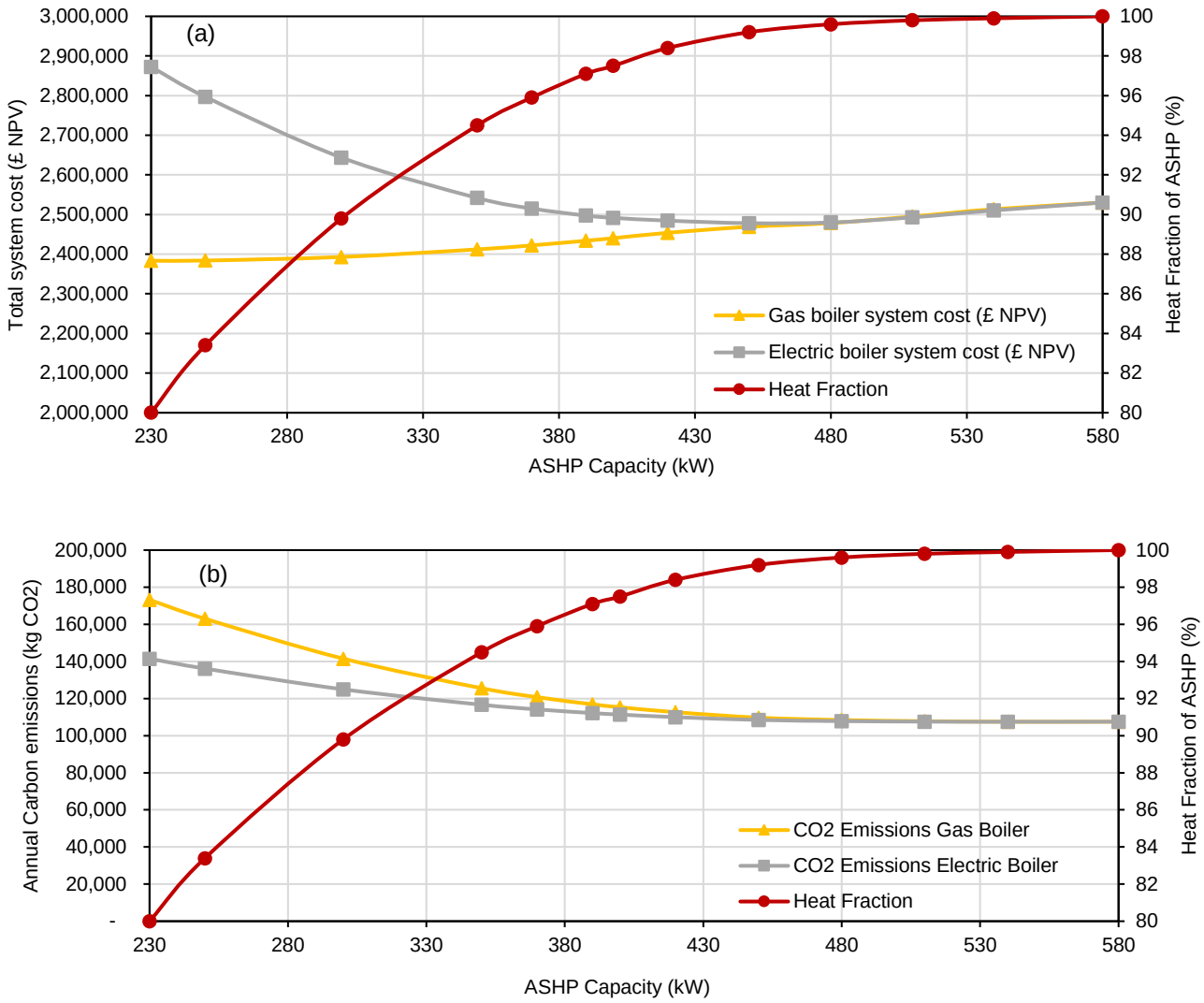

Figure 5 – (a) and (b), NPV and carbon emissions of electric and gas boilers with increasing ASHP size.

As heat pump size increases, heat fraction increases at a diminishing rate. Above a 98% heat fraction, the model shows that the ASHP must increase by a further 40% to be able to supply the full heat requirement.

When providing 20% of the heat, gas boilers provide the lowest total cost, but also the highest carbon. Electric boilers present the highest cost solution at 20% due to the large electricity demand and costs.

As the heat fraction of the heat pump increases, the total system costs reduce for electric boilers and increase for gas boilers until c. 95-97% heat fraction where there is very little cost or carbon difference between the two boiler technologies.

Upwards of 98-99% heat fraction, there is almost no net reduction in carbon emissions and the costs increase for both technologies due to the large heat pump capacity required to achieve 100% heat fraction.

For lower heat fractions, a gas boiler would be the best investment, but for a small increase in total costs and heat tariff, a higher heat fraction (c.95%) can be achieved which would allow transition to an electric boiler and ensure significantly lower carbon emissions and complete removal from the gas grid.

It should be noted that the costs associated with being connected to the gas grid and the electrical connection upgrade costs will be significantly variable factors for different projects which are not included in the above analysis. These should be considered on a case-by-case basis.

3.5. Effect of changing demand profiles

The effect of changing the demand profiles using the same scheme size was investigated on all schemes and found not to affect any of the above conclusions for increasing PV, solar thermal, ASHP or the difference between electric and gas boilers.

The most significant impact of note was the size of the heat pump required to achieve a certain heat fraction in each demand profile. This is shown below in Figure 6.

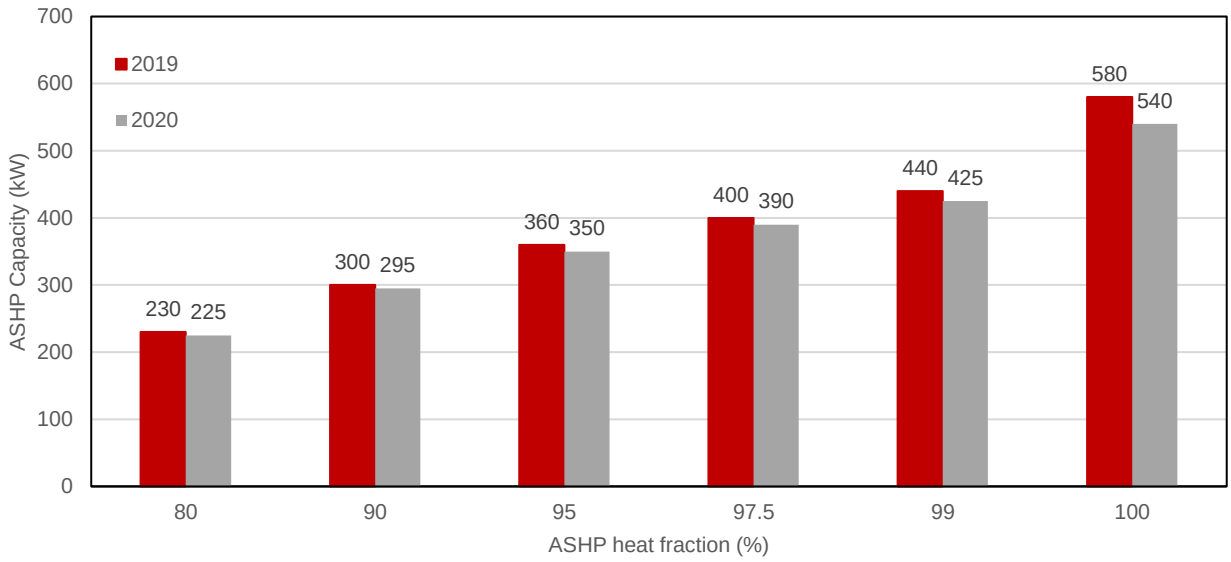

Figure 6 – Effect of demand profile on heat pump size required.

Whilst there is only a small increase for most heat fractions the size of increase required increases with increasing heat fraction. This effect is due to the larger size of the peaks in the demand profile which require a larger heat pump size to overcome.

It should also be noted that since the profile is hourly, the peak demands are averaged over the hour and therefore will not be as large as they would if the data were 5 or 15-minute averaged. This would indicate an even bigger increase in ASHP size.

Other findings include that, solar thermal heat fractions increased by 1% when using the 2020 profile due to shallower peaks and therefore improved ability for solar thermal storage to be used.

3.6. Effect of scheme size

The effect of changing the scheme size was investigated on all above scenarios and found not to affect any of the above conclusions for increasing PV, solar thermal, ASHP or the difference between electric and gas boilers.

The alteration of scheme size did however reveal the extent to which solar thermal is limited by space availability and its comparative load size, Table 11 details the calculated heat fractions for a full roof array on different schemes and the size increase required to provide an arbitrary 20% heat fraction. The thermal store size has not been changed from that detailed in Table 3.

Location	**Dwellings**	**Annual demand (kWh)**	**Available roof space (on single roof)**	**Solar thermal fraction (%)**	**Roof space required for 20% fraction (m^2)**	**Percentage increase required (%)**
Tower Hamlets	100	451,660	625	13.90	906	45%
Southwark	200	1,043,480	600	6.70	1,845	208%
Newham	350	1,580,820	1,020	6.50	3,354	229%
Newham	500	2,258,310	450	2.10	4,696	944%
Kingston upon Thames	1,000	4,516,620	940	1.90	11,524	1,126%

Table 11 – influence of scheme size and roof space availability on solar thermal heat fraction.

On smaller schemes, solar thermal has a reasonable influence on heat fraction because the roof space is relatively large compared to the demand size. However, for larger schemes, as the solar thermal array has been constrained to one rooftop for the purpose of minimising piping and controls cost, the heat fraction becomes almost insignificant.

This trend is repeated in the amount of roof space required to provide a 20% heat fraction showing the scale of the area requirement on larger schemes.

it is estimated that increased thermal storage would reduce the area requirement to go above the 20% heat fraction but this has not been modelled and economies of scale would become significant when examining the total system cost.

For all rooftop scale arrays modelled, the total system costs always increased when solar thermal was added in contrast to when PV is added. This is mainly due to cost and the fact that PV reduces the cost of electricity more than solar thermal does which is the controlling influence on OpEx.

4.0 Conclusions

This paper has investigated the technoeconomic opportunities for using different supplemental technologies on heat pump-led heat networks in London. The effect of scheme size and demand profile representing pre and mid pandemic behaviour from 2019 and 2020 respectively has also been investigated to determine the robustness of each supplemental technology. The main conclusions are as follows:

- Increasing PV array size reduced total system cost until utilisation reached less than c.40% on all scheme sizes. As the utilisation never fell this low on any size scheme, the increase in CapEx was always paid for over 30-years by the reduction in OpEx, however the additional CapEx was not paid for by the reduction in GLA carbon offset payments and so a developer may be reluctant to add this additional cost.
- Increasing solar thermal array size on any scheme size did not reduce total system cost in any model on any scheme size, unlike PV. This is because solar thermal has a larger impact on reducing ASHP heat fraction than boiler heat fraction, and as a result has a lesser effect on reducing electricity costs than PV does.
- Increasing ASHP capacity gives the highest carbon emissions reduction for the lowest cost due to reducing carbon offsetting costs between 80% to 95% heat fractions.
- In the region of 95-98% ASHP heat fraction, the transition from gas to electric boiler has very little effect on NPV or carbon emissions and would be recommended to completely electrify heat supply.
- Combining ASHP and electric boilers at a >95% ASHP heat fraction with rooftop PV would provide the most optimal carbon and cost reductions on any of the schemes modelled.
- The DHW profile in 2020 showed a dramatically reduced weekday morning peak than in 2019. This could be attributed to the effect of COVID-19 and greater flexibility in demand due to additional time spent at home. The result of these profiles did not significantly affect any of the above conclusions but if the 2020 profiles were used, the ASHP size at any heat fraction could be reduced. The effect of this was biggest at 100% heat fraction which gave a 6% reduction in peak capacity.
- Scheme size was not found to affect the above conclusions and mainly indicated the importance of space availability and thermal storage for optimal solar thermal use. This cannot be verified on schemes larger than 1000 dwellings as economies of scale will become significant.

It is clear that where heat pumps are the central generation technology in a hybrid system, the heat fraction of the heat pump should be maximised first with respect to the project budget constraints. The choice between gas or electric boiler will then depend on the resulting heat fraction. Subsequent to this decision, PV can be added to counterbalance electricity costs and have a positive impact on lifetime cost and, particularly, the cost of delivered heat which solar thermal cannot achieve.

5.0 References

[1] CCC, *The Sixth Carbon Budget: The UK's path to Net Zero,* London, UK: The Climate Change Committee, 2020.

[2] P. Jones, P. Woods and M. Crane, *CP1 Heat Networks: Code of Practice for the UK, Raising the standards of heat supply, 2nd Edition,* London, UK: CIBSE, ADE, 2020.

[3] GLA, *The London Plan, The Spatial Development Strategy for Greater London,* London: Mayor of London, Greater London Authority (GLA), March 2021.

[4] *The Building Regulations 2010, Approved Document L1A: Conservation of fuel and power in new dwellings,* London, UK: NBS, RIBA for HM Government, 2013 edition incorporating 2016 amendments.

[5] *The Building Regulations 2010, Approved Document L2A: Conservation of fuel and power in new buildings other than dwellings,* London, UK: NBS, RIBA for HM Government, 2013 edition incorporating 2016 amendments.

[6] BEIS, *Solar Photovoltaics Deployment in the UK - National Statistics,* London, UK: Department for Business, Energy & Industrial Strategy, February 2021.

[7] D. Tschopp, Z. Tian, M. Berberich, J. Fan and B. Perers, "Large-scale solar thermal systems in leading countries: A review and comparative study of Denmark, China, Germany and Austria," *Applied Energy,* vol. 270, no. ISSN 114997, 2020.

[8] CIBSE, "CIBSE Weather data (I)," 2021. [Online]. Available: https://www.cibse.org/knowledge/weather-data-(1). [Accessed 07 June 2021].

[9] BEIS, *SAP 10.1 - The Government's Standard Assessment Prcedure for Energy Rating of Dwellings, Version 10.1,* London, UK: Building Research Establishment (BRE), 2019.

[10] BESA, "UK HIU Test Regime Technical Specification," BESA Publications, Penrith, 2018.

[11] B. Y. H. Liu and R. C. Jordan, "The Long-Term Average Performance of Flat-Plate Solar-Energy Collectors," *Solar Energy,* vol. 7, no. 2, pp. 53-74, 1963.

[12] P. Ineichen, R. Perez and R. Seals, "The importance of correct albedo determination for adequately modeling energy received by tilted surfaces," *Solar Energy,* vol. 39, no. 4, pp. 301-305, 1987.

[13] S. Moslehi, T. Reddy and S. Katipamula, “Evaluation of scenario-specific modeling approaches to predict plane of array solar irradiation,” *Science and Technology for the Built Environment,* vol. 24, no. 7, pp. 770-778, 2018.

[14] *BS EN 12975-2:2006 Thermal solar systems and components - Solar collectors. Test methods,* Brussels, Belgium: European Committee for Standardization, 2006.

[15] *ASHRAE Standard 77-93: Methods of Testing to Determine the Thermal Performance of Solar Collectors,* Washington DC, USA: American Society of Heating, Refrigerating and Air-Conditioning Engineers, 1997.

[16] *BS EN ISO 9806: Solar energy - solar thermal collectors - test methods,* Brussels: European Committee for Standardization, 2017.

[17] J. A. Duffie and W. A. Beckman, Solar Engineering of Thermal Processes - 4th Edition, Hoboken, New Jersey: John Wiley & Sons, 2013.

[18] GSA, “globalsolaratlas.info,” 2021. [Online]. Available: https://globalsolaratlas.info/support/methodology. [Accessed 24 April 2021].

[19] HOMERPro, “www.homerenergy.com,” 2021. [Online]. Available: https://www.homerenergy.com/products/pro/docs/latest/how_homer_calculates_the_pv_cell_temperature.html. [Accessed 27 April 2021].

[20] BEIS, *Solar PV cost data, taken from the Microgeneration Certification Scheme (MCS) installation database,* London, UK: Department for Business, Energy & Industrial Strategy (BEIS), 2020.

[21] BEIS, *Quarterly Energy Prices, Quarter 4 2020 - National Statistics,* London, United Kingdom: Department for Business, Energy & Industrial Strategy, 2021.

[22] A. Walker, E. Lockhart, J. Desai, K. Adriani, G. Klise, O. Lavrova, T. Tansy, J. Deot, B. Fox and A. Pochiraju, *Model of Operation-and-Maintenance Costs for Photovoltaic Systems,* National Renewable Energy Laboratory, Sandia National Laboratories, SunSpec Alliance, June, 2020.

[23] IRENA, *Renewable Power Generation Costs in 2019,* Abu Dhabi: International Renewable Energy Agency (IRENA), 2020.

[24] BEIS, *2018 Updated Energy & Emissions Projections, Annex M - growth assumptions and prices,* London, UK: Department for Business, Energy and Industrial Strategy (BEIS), 2019.

Acronyms/Abbreviations

AHU	Air Handling Unit
AM	Air Mass
AOI	Angle of Incidence
ASHP	Air Source Heat Pump
BHI	Beam Horizontal Irradiation
BOS	Balance of System
CapEx	Capital Expenditure
CCC	Climate Change Committee
COP	Coefficient of Performance
DHI	Direct Horizontal Irradiation
DHW	Domestic Hot Water
DNI	Direct Normal Irradiation
GHI	Global Horizontal Irradiation
GLA	Greater London Authority
GSHP	Ground Source Heat Pump
GTI	Global Tilted Irradiation
HIU	Heat Interface Unit
HP	Heat Pump
IAM	Incidence Angle Modifier
LeTID	Light and Elevated Temperature Induced Degradation
LTHW	Low Temperature Hot Water
MPP	Maximum Power Point
NOCT	Nominal Operating Cell Temperature
NPV	Net Present Value
OpEx	Operating Expenditure
PHE	Plate Heat Exchanger
PV	Photovoltaics
SCOP	Seasonal Coefficient of Performance
STC	Standard Test Conditions (25°C, 1000 W/m^2, AM 1.5)
TRY	Test Reference Year
TS	Thermal Store

Nomenclature

A	Collector aperture area	(m^2)
a_1	First order heat loss factor	(W/m^2.K)
a_2	Second order heat loss factor	(W/m^2.K)
C_{eff}	Thermal capacity of collector	(J/m^2.K)
CF_n	Cash flow in year	(£)
COP_{HP}	Heat pump coefficient of performance	(Dimensionless)
GCF_{SAP}	Gas carbon factor	(kg CO_2/ kWh)
ECF_{SAP}	Electricity carbon factor	(kg CO_2/ kWh)

i	Discount rate	(%)
I_B	Beam horizontal irradiation	(W/m^2)
I_D	Diffuse horizontal irradiation	(W/m^2)
I_{GHI}	Global horizontal irradiation	(W/m^2)
I_{GTI}	Global tilted irradiation	(W/m^2)
I_{STC}	Incident irradiation under STC	(1000 W/m^2)
$I_{T,NOCT}$	Irradiation at which NOCT is calculated	(800 W/m^2)
K_θ	Average incidence angle modifier	(Dimensionless)
n	Number of years	(years)
P_{ANC}	Energy centre ancillary power consumption	(W)
P_{EB}	Electric boiler power consumption	(W)
P_{HP}	Heat pump power consumption	(W)
P_{PV}	PV power output	(W)
P_{nom}	Nominal PV power output at STC	(W)
Q_{EB}	Electric boiler heat output	(W)
Q_{GB}	Gas boiler heat output	(W)
Q_{HP}	Heat pump heat output	(W)
Q_{ST}	Solar collector heat output	(W)
R_B	Beam geometric factor	(Dimensionless)
R_D	Diffuse geometric factor	(Dimensionless)
R_R	Reflection geometric factor	(Dimensionless)
T_a	Ambient temperature	(°C)
$T_{a,NOCT}$	Ambient temperature at which NOCT is calculated	(20°C)
$T_{C,NOCT}$	Nominal operating cell temperature	(°C)
$T_{C,STC}$	PV cell temperature under STC	(25°C)
T_C	PV cell temperature at each time step	(°C)
T_m	Mean collector temperature	(°C)
α_p	Power temperature coefficient at P_{nom}	(%/°C)
α_s	Solar altitude	(°)
β	Panel tilt	(°)
γ	Panel azimuth	(°)
γ_s	Solar azimuth	(°)
η_{EB}	Electric boiler efficiency	(%)
η_{GB}	Gas boiler efficiency	(%)
η_o	Optical efficiency of solar collector	(%)
$\eta_{mp,STC}$	PV efficiency at MPP under STC	(%)
θ	Angle of incidence	(°)
θ_z	Solar zenith	(°)
ρ_g	Albedo coefficient	(Dimensionless)
$\tau\alpha$	Transmittance and Absorptance	(%)